PRESSURE DISTRIBUTION ASSESSMENTS FOR A PRIMARY BEAM OF A FLAT WIPER

D.-C. Huang[1], M.-R. Zhang[2], Z.-Q. Huang[2], K.-C. Liao[1*]
[1]Department of Bio-Industrial Mechatronics Engineering
National Taiwan University
No. 1, Sec. 4, Roosevelt Road, Taipei 10617, Taiwan
[2]Sandolly International Corporation
No.26, Huadong Rd, Kaohsiung 83162, Taiwan
[*]E-mail address: kokki@ntu.edu.tw

ABSTRACT

Recently standard wiper blades have been gradually replaced by flat wiper blades due to several advantages such as simple structures. A schematic approach is developed to appraise the suitability of the geometry of a metallic beam, one of major components of the flat wipe blade, in the present study. The beam is compressed against a level surface via a rocker arm mechanism, and the corresponding pressure distribution under the beam is measured by using piezoelectric sensors. Pressure distributions along the longitudinal direction of the beam based on the numerical simulations are in good agreement with those based on the experiments. A parameterized beam model is proposed here to achieve anticipated characteristics of the pressure distributions of the beam provided. Three geometric parameters built in a computer-aided drawing (CAD) model are investigated to evaluate their influences on the pressure distributions of the beam. An optimization software linked to CAD software and a finite element analysis software is further adopted based on various self-defined optimization indexes to search for an ideal parameter combinations. The suggested geometry of the beam is then sampled to validate the appropriateness of the current pressure assessment procedures.

Key Words: flat wiper, pressure distribution, finite element analysis

1. Introduction

A wiper system applied to a windshield is a crucial device securing clear sight for drivers. Pressure distributions along the longitudinal direction of the wiper blade subjected to the compressive loading conditions are commonly adopted for the assessment of its performance. Uniform pressure distributions are always expected but virtually unable to be attained realistically. Grenouillat and Leblanc, 2002 proposed a mathematical model based on elastic foundations theory to efficiently estimate the pressure distributions of a standard wiper blade against both a flat glass and a windshield under various loads. Calculation results agree fairly with the corresponding experimental measurements. Lee *et al.*, 2002 numerically examined effects of several design features on the pressure distributions of the standard wiper blade on a flat glass. They concluded that the pressure distribution is relatively sensitive to the curvature of the primary beam, the rotational angle of the yoke, and the thickness of the steel beam. Nevertheless no experimental validations were reported in the study of Lee *et al.* Kim *et al.*, 2002 developed a continuum-based shape design sensitivity formulation for the hyperelastic material with multibody frictional contact. The proposed algorithm was implemented into the optimization process for the cross-section of a rubber blade. Optimized geometry based on several performance measures was determined with less computational effort.

Demands of the flat wiper blade with two major components of a metallic beam and a rubber blade, having a rather simple structure in comparison with the standard wiper blade, grow rapidly in recent years. Based on the authors' understanding, there are few research studies related to the flat wiper blade. A finite element analysis is carried out

to investigate effects of the beam geometry on the pressure distribution of the beam loaded on a level surface here. A parameterized beam model is suggested and optimization procedures for the anticipated pressure distribution are constructed. Pressure distributions based on two representative indexes are then demonstrated and verified experimentally.

2. Materials and methods

2.1 Experiments

In the current preliminary study, stainless beams were compressed against the level surface instead of a windshield to obtain the corresponding pressure distribution by utilizing piezoelectric sensors. A schematic of the experimental set-up and the associated components were labeled as shown in Fig. 1. Per specification requirements, the beam demands to be subjected to 1.0 – 1.4 grams per millimeter in longitudinal length. Here 840 grams was chosen to be loaded on the 600-millimeter-long beam. A piezoelectric sensor with 128 sensing units was placed under the beam. An arm mechanism was then released to prescribe the loading on the middle length position of the beam. Compression force was able to be altered to reach the target magnitude by using an electronic scale and by adjusting the length of a spring embedded in the arm mechanism. Signal of each sensing unit was transformed into the pressure measurement through a data acquisition device.

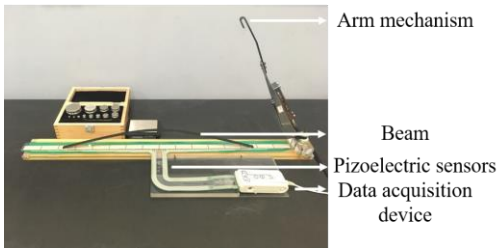

Fig. 1 A schematic of the experimental set-up

2.2 Numerical simulations

A widely-used finite element commercial package Abaqus (Dassault Systèmes Simulia Corp., 2016) is utilized to examine the pressure distributions of the beam. Fig. 2 shows the analysis model comprising of the beam, the level surface, and the rocker arm. Since the stainless beam under the force of 840 grams is still within the range of elastic deformation, only Young's modulus of 210 GPa and Poisson's ratio of 0.3 are adopted in the calculations. For the sake of simplicity, the level surface is considered as a rigid body without sacrificing the numerical accuracy. In order to compare the simulated pressure distributions with the corresponding measurements of 128 sensing units, the level surface is therefore divided into 128 regions with the same size as each unit. Note that the total reaction force divided by the total area of the individual region is regarded as the predicted pressure. The arm mechanism includes a spring element (as shown in the insert of Fig. 2) used to vary the compression force loaded on the beam. To practically estimate the pressure distributions of the beam in the wiper industry, the compression force of the arm against the curved windshield is first tuned to the expected value at the specific location/orientation as displayed in Fig. 3. Without any further adjustment, compression forces at other locations/orientations thus depend upon variations of the curvature of the windshield. It is worthy to be noted that the present developed arm mechanism can be applied to both the level surface and the windshield as well. Two contact pairs are set between the end of the arm and the top surface of the beam and the level surface and the bottom surface of the beam.

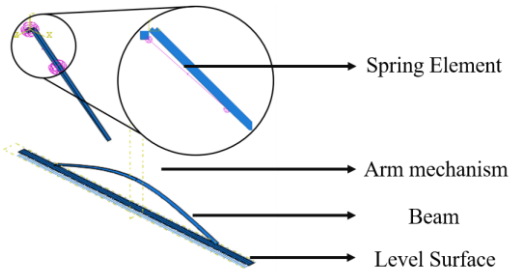

Fig. 2 Numerical analysis model

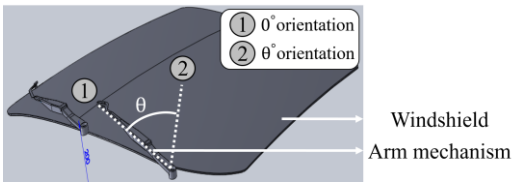

Fig. 3 A schematic of the compression force estimation on windshield

It is well known that the beam geometry significantly influences the associated pressure distributions. A parameterized beam model with three parameters (A, B, and D, not shown here for the confidential issue) is then built by using a three-dimensional computer-aided drawing (CAD) software Solidworks (Dassault Systèmes SolidWorks Corp., 2016). An optimization software Isight (Dassault Systèmes Simulia Corp. 2016) linked to Solidworks (Dassault Systèmes SolidWorks Corp., 2016) and Abaqus (Dassault Systèmes Simulia Corp., 2016) is further adopted to search for ideal parameter combinations. A flowchart of the optimization procedures is demonstrated in Fig. 4.

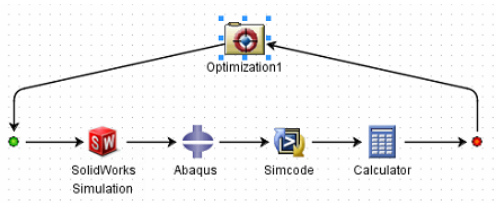

Fig. 4 A flowchart of the optimization procedures

The analysis model with initial values of three parameters built in Solidworks (Dassault Systèmes SolidWorks Corp., 2016) is imported into Abaqus (Dassault Systèmes Simulia Corp., 2016) to assess the pressure distributions of the beam. Simulated physical fields are extracted by Simcode module of Isight (Dassault Systèmes Simulia Corp., 2016), and various self-defined optimization indexes are evaluated by using Calculator module. New values of parameters are determined via the Hooke-Jeeves algorithm and introduced into Solidworks (Dassault Systèmes SolidWorks Corp., 2016) again. Above procedures will be repeated until the setting iteration number is reached. Based on the authors' knowledge, as shown in Fig. 5(a) and 5(b), performances of the pressure continuity and the pressure outward expansion of the beam are typically required. Two indexes, IND1 and IND2, are then proposed to respectively characterize the pressure continuity and the outward expansion.

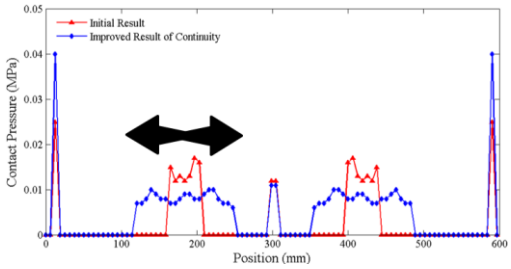

Fig. 5(a) Improvement of the pressure continuity

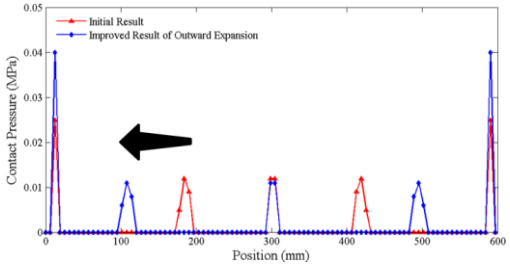

Fig. 5(b) Improvement of the pressure outward expansion

2.3 Results and discussion

Fig. 6 shows comparisons of the pressure distribution along the longitudinal direction of the beam based on the experiments and the simulations. Note that the range of the abscissa in the figure is 800 mm due to the length of the piezoelectric sensor. It is remarked that the pressure peak locations based on the numerical analysis are in fair agreement with those based on the measurements even though the estimated magnitudes of the pressure are in general smaller than the measured ones.

Nine sets of aforementioned A, B, and D are selected first to appraise effects of these parameters on the pressure performance. As illustrated in Fig. 7, a number of the pressure peak increases as a ratio of A to B rises with A=15. Furthermore the performance of the pressure continuity is best among these parameter combinations under the condition of A=15/B=10/D=80, while the pressure peak significantly expands outwards under the condition of A=20/B=20/D=80. The combination of A=15/B=15/D=80 is arbitrarily chosen as initial values of three parameters for the following optimization procedures. As described above, two indexes IND1 and IND2 are suggested to examine variations of the pressure distribution whether

the pressure continuity and outward expansion can be reached.

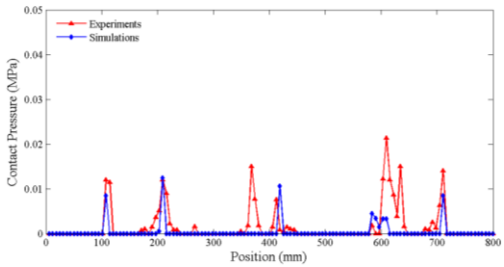

Fig. 6 Comparisons of the pressure distribution based on the experiments and the simulations

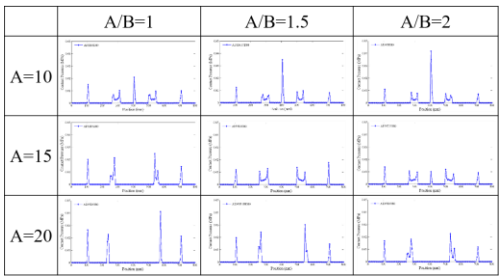

Fig. 7 Simulated pressure distributions based on nine sets of A, B, and D

Figs. 8(a) and 8(b) respectively show the simulated pressure distributions under the optimization procedures based on IND1 and IND2. The pressure continuity based on A=5/B=5/D=87 evidently increases after the optimization procedures compared with that based on A=15/B=15/D=80 (initial values of the parameter) as shown in Fig. 8(a). Moreover Fig. 8(b) displays that the outward expansion of the pressure peak towards the end of the beam based on A=22/B=19/D=85 is more significant than that based on A=15/B=15/D=80. Pressure distributions of the practically sampled beams according to the above optimization results are then further measured. CAD models of the beams via the reverse-engineering technology are also generated. Fig. 9 illustrates the pressure distributions of the sampled beam, the CAD model of the beam via the reverse-engineering technology (RET), and the CAD model of the beam based on various parameter combinations. Differences between the pressure distributions of the CAD model of the beam and that via the RET can be attributed to the manufacturing processes. Mismatched pressure distributions of the CAD model of the beam via the RET and the sampled beam are regarded as the differences between the simulation results and the measurements. Generally the pressure distributions based on the CAD model via the RET are in fair agreement with those based on the sampled beam. Figs. 9(b) and 9(c) respectively confirm that the pressure continuity based on A=5/B=5/D=87 and the pressure outward expansion based on A=22/B=19/D=85 can be significantly improved. Nonetheless combinations of these two indexes with different weighting factors or new indexes should be advised to simultaneously retain the pressure continuity and outward expansion in the near future.

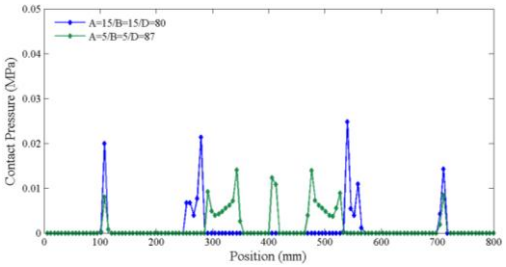

Fig. 8(a) Simulated pressure distributions under the optimization procedures based on IND1

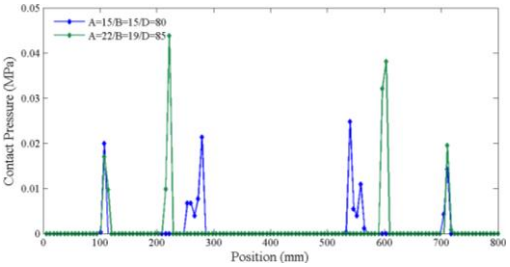

Fig. 8(b) Simulated pressure distributions under the optimization procedures based on IND2

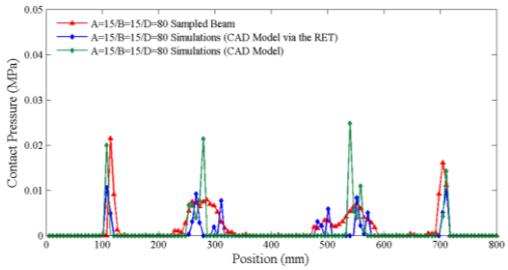

Fig. 9(a) Pressure distributions of the sampled beam, the CAD model of the beam via the reverse-engineering technology, and the CAD model of the beam based on A=15/B=15/D=80

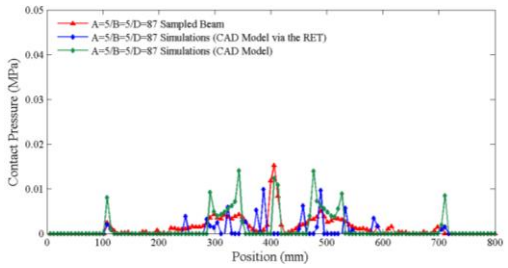

Fig. 9(b) Pressure distributions of the sampled beam, the CAD model of the beam via the reverse-engineering technology, and the CAD model of the beam based on A=5/B=5/D=87

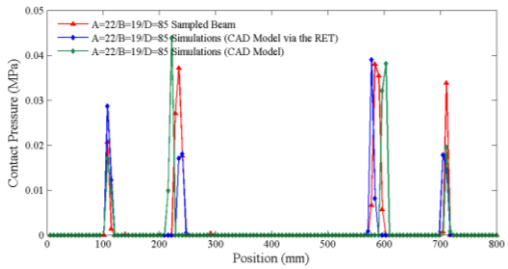

Fig. 9(c) Pressure distributions of the sampled beam, the CAD model of the beam via the reverse-engineering technology, and the CAD model of the beam based on A=22/B=19/D=85

3. Conclusions

Pressure distributions of the beam of the flat wiper blade on the level surface based on the simulations match fairly with those based on the measurements. The optimization procedures connecting the three-dimensional drawing, the finite element analysis, and the optimization commercial packages are proposed to finalize the appropriate beam geometry. Experiments validate that the pressure distributions of the optimized beam based on various indexes indeed exhibit the designated characteristics. Whole processes presented in this study can be further extended to assess the performance of the beam on the windshield.

4. References

[1] Dassault Systèmes Simulia Corp. 2016. ABAQUS/Standard v.2016 SE. Johnston, Rhode Island.

[2] Dassault Systèmes Simulia Corp. 2016. Isight SIMULIA. 2016. Johnston, Rhode Island.

[3] Dassault Systèmes SolidWorks Corp. 2016. Solidworks 2016.Concord, Massachusetts.

[4] Grenouillat, R. and C. Leblanc, "Simulation of Mechanical Pressure in a Rubber-Glass Contact for Wiper Systems," SAE Technical Paper Series, 2002, 2002-01-0798.

[5] Kim, N. H., Y. H. Park and K. K. Choi, "Optimization of a Hyper-elastic Structure with Multibody Contact Using Continuum-based Shape Design Sensitivity Analysis," Struct Multidisc Optim 21, 2001, 196–208.

[6] Lee, S. H., Y. H. Kim, J. Sung, K. C. Shin and J. H. Oh, "Investigation of the Contact Force Distribution and Dynamic Behaviour of an Automobile Windshield Wiper Blade System," Proceedings of the Institution of Mechanical Engineers, Part D: Journal of Automobile Engineering 227, 2013, 1040–1052.